Biomedicine & Pharmacotherapy 144 (2021) 112317

Contents lists available at ScienceDirect

Biomedicine & Pharmacotherapy

journal homepage: www.elsevier.com/locate/biopha

# pH-responsive and folate-coated liposomes encapsulating irinotecan as an alternative to improve efficacy of colorectal cancer treatment

Shirleide Santos Nunes [a], Sued Eustaquio Mendes Miranda [a], Juliana de Oliveira Silva [a], Renata Salgado Fernandes [a], Janaína de Alcântara Lemos [a], Carolina de Aguiar Ferreira [b], Danyelle M. Townsend [c], Geovanni Dantas Cassali [d], Mônica Cristina Oliveira [a], André Luís Branco de Barros [e,*]

[a] Department of Pharmaceutical Products, Faculty of Pharmacy, Universidade Federal de Minas Gerais, Av. Antônio Carlos, 6627, 31270-901 Belo Horizonte, Minas Gerais, Brazil
[b] Department of Medical Physics, University of Wisconsin-Madison, Madison, WI 53705, USA
[c] Department of Drug Discovery and Pharmaceutical Sciences, College of Pharmacy, Medical University of South Carolina, USA
[d] Department of General Pathology, Institute of Biological Sciences, Universidade Federal de Minas Gerais, Av. Antônio Carlos, 6627, 31270-901 Belo Horizonte, Minas Gerais, Brazil
[e] Department of Clinical and Toxicological Analyses, Faculty of Pharmacy, Universidade Federal de Minas Gerais, Av. Antônio Carlos, 6627, 31270-901 Belo Horizonte, Minas Gerais, Brazil

ARTICLE INFO

*Keywords:*
Liposomes
Irinotecan, polyethylene glycol
Antitumor activity
Folate-coated

ABSTRACT

Irinotecan (IRN) is a semisynthetic derivative of camptothecin that acts as a topoisomerase I inhibitor. IRN is used worldwide for the treatment of several types of cancer, including colorectal cancer, however its use can lead to serious adverse effects, as diarrhea and myelosuppression. Liposomes are widely used as drug delivery systems that can improve chemotherapeutic activity and decrease side effects. Liposomes can also be pH-sensitive to release its content preferentially in acidic environments, like tumors, and be surface-functionalized for targeting purposes. Herein, we developed a folate-coated pH-sensitive liposome as a drug delivery system for IRN to reach improved tumor therapy without potential adverse events. Liposomes were prepared containing IRN and characterized for particle size, polydispersity index, zeta potential, concentration, encapsulation, cellular uptake, and release profile. Antitumor activity was investigated in a murine model of colorectal cancer, and its toxicity was evaluated by hematological/biochemical tests and histological analysis of main organs. The results showed vesicles smaller than 200 nm with little dispersion, a surface charge close to neutral, and high encapsulation rate of over 90%. The system demonstrated prolonged and sustained release in pH-dependent manner with high intracellular drug delivery capacity. Importantly, the folate-coated pH-sensitive formulation had significantly better antitumor activity than the pH-dependent system only or the free drug. Tumor tissue of IRN-containing groups presented large areas of necrosis. Furthermore, no evidence of systemic toxicity was found for the groups investigated. Thus, our developed nanodrug IRN delivery system can potentially be an alternative to conventional colorectal cancer treatment.

## 1. Introduction

Camptothecins are efficient antineoplastic alkaloid-derived compounds that belong to the family of the topoisomerase I interactive substances [1]. Topotecan and irinotecan (IRN) are two camptothecins that have already been approved by the US Food and Drug Administration (FDA) [1,2]. IRN (7-Ethyl-10-(4-[1-piperidino]-1-piperidino) carbonyloxycamptothecin) is a first-line drug approved for the treatment of a variety of cancer types, including colorectal, lung, and gynecological cancers [3]. While it can be used as a monotherapy, it is usually administered in combination with cytotoxic agents, including oxaliplatin and 5-fluorouracil (5-FU) and as a rescue therapy in 5-FU-refractory disease [4,5]. The primary target, Topo1 is ubiquitously expressed and consequently the drug has been shown to have serious side effect with

* Correspondence to: Faculty of Pharmacy, Federal University of Minas Gerais, Av. Antônio Carlos, 6627, 31270-901 Belo Horizonte, Minas Gerais, Brazil.
*E-mail addresses:* brancodebarros@yahoo.com.br, albb@ufmg.br (A.L. Branco de Barros).

https://doi.org/10.1016/j.biopha.2021.112317
Received 9 September 2021; Received in revised form 29 September 2021; Accepted 6 October 2021
Available online 8 October 2021

large inter-individual variability. The toxicities associated with IRN include myelosuppression (neutropenia) and gastrointestinal disorders (mainly diarrhea), which are recognized as constituting dose-limiting toxicity for this drug [4,6].

IRN is a prodrug which has a complex pharmacologic profile and is extensively metabolized in vivo. Metabolism in the gastrointestinal tract occurs in three major steps starting with the conversion of water-soluble IRN to generate the potent metabolite SN-38 (7-ethyl-10-hydroxycamptothecin). In the second step, SN-38 is metabolized to a glucuronide which can be exported to the intestine and reactivated to its toxic form by bacterial β-glucuronidase where it can be reabsorbed. The local reactivation of the drug in the intestinal tract is attributed to its toxicity [7].

Efforts to identify biomarkers to determine which patient population will be more impacted has not been successful. Consequently, alternative platforms for delivery are a viable option that can incorporate precision medicine into the drug delivery system. This notion is further supported by the complex pharmacokinetic profile of the drug following intravenous administration [8]. SN-38 has 100- to 1000-fold more potent antitumor effects, however, after intravenous administration of free IRN, only less than 5% of IRN is converted to SN-38, mainly in the liver. The most active form of camptothecin contains an open lactone configuration, which is formed through an esterification reaction in the presence of the enzyme carboxyl esterase. Carboxyl esterase is present in all tissues, including tumors [3,9] and it is more prominent in acidic environments. In this context, IRN pharmacokinetic profile would greatly benefit from a tool that can protect and stabilize IRN and enable its conversion to the most active metabolite more specifically in the tumor tissue.

Nanoparticle-based drug delivery systems have emerged as promising tools to alter pharmacokinetic profile of drugs [8–10]. More specifically, drug delivery strategies focused on the stabilization of the lactone ring of IRN to avoid its inactivation have been previously reported. Liposomes are considered to be one of the most promising drug delivery systems designed to encapsulate a wide range of drugs and provide suitable strategies to improve the efficacy of chemotherapeutics in cancer treatment [11–13]. Encapsulating a drug into liposomes is highly advantageous as it can improve its pharmacokinetics, promote its intracellular uptake, and allow selective delivery to tumor cells, often resulting in decreased undesirable side effects and increased maximum tolerated dose [14,15].

Several strategies have been explored to improve the pharmacokinetics and targeting of liposomal formulations to further optimize the activity/toxicity of encapsulated drugs [4]. Our research group has successfully employed long-circulating pH-sensitive liposomes (SpHL) for treatment of several types of solid tumors [16–20]. To the best of our knowledge, we will describe, for the first time, the use of pH-sensitive liposomes encapsulated with IRN for treatment of colorectal cancer. Our approach is founded in knowledge that the tumor environment normally has a lower pH than normal tissues. Such acidic conditions will promote cellular uptake of SpHL via endosome formation and allow local targeted drug release in the tumor [16,21].

Furthermore, the use of nanoparticles such as liposomes can leverage tumor specificity through the addition of surface molecular markers for tumor targeting and accumulation [22–25]. Folate, for example, is a molecule used in different metabolic cycles during amino acid synthesis to support and promote cell growth. Folate receptor is overexpressed in the tumor environment while only minimally distributed in normal tissues, resulting in an optimal targeting approach. Functionalization of liposomes with folate is a great tumor targeting strategy that can further improve its pharmacokinetic profile and potential drug antitumor activity [26,27].

Herein, we have developed a novel liposome-based targeted drug delivery system as a tool to improve IRN tumor therapy efficiency with low toxicity profile. The development and characterization of controlled release pH-sensitive liposomes encapsulated with IRN was carried out and investigated as a promising anti-tumor agent in a murine model of colorectal cancer.

## 2. Material and methods

### 2.1. Materials

Trihydrated irinotecan hydrochloride (IRN) was donated from EUROFARMA Laboratórios SA (São Paulo, Brazil). The dioleoylphosphatidylethanolamine (DOPE), and distearoylphosphatidylethanolamine polyethyleneglycol2000 (DSPE-PEG2000/DSPE-PEG-FOL) were supplied by Lipoid GmbH (USA). Cholesteryl hemisuccinate (CHEMS) and cholesterol (CHOL) were purchased from Sigma-Aldrich Chemical Company (St Louis, USA). Glucose was purchased from Vetec Química Fina Ltda (São Paulo, Brazil). All solvents (high-performance liquid chromatography analytical grade) and other reagents were purchased from Sigma-Aldrich (São Paulo, Brazil). The subcutaneous tumor model was established in 8–10- week-old female BALB/c mice purchased from CEBIO-UFMG (Belo Horizonte, Brazil). Animals were kept under SPF condition with free access to standard food and water. All animal studies were approved by the local Ethics Committee for Animal Experiments of Federal University of Minas Gerais, Brazil (protocol # 102/2020).

### 2.2. Methods

#### 2.2.1. Liposome preparation

Liposomes were prepared according to the lipid film hydration method [28], followed by size calibration. Briefly, chloroform aliquots of DOPE, CHEMS, DSPE-PEG2000 (5.8:3.7:0.5 molar ratio, respectively; total lipid concentration was equal to 40 mM) or DOPE, CHEMS, DSPE-PEG2000, and DSPE-PEG2000-Fol (5.8:3.7:0.45:0.05 molar ratio, respectively; total lipid concentration was equal to 40 mM) were transferred to a flask and the solvent was removed at low pressure to prepare SpHL and SpHL-Fol, respectively. Aliquots of 0.1 M NaOH solution were added to lipid film to promote complete ionization of CHEMS molecules, and subsequently, the formation of a lamelar structure. Then, lipid film was hydrated with 300 mM ammonium sulfate solution, at room temperature, under vigorous stirring [29]. The liposomes obtained were calibrated by extrusion using polycarbonate membranes of 0.4 μm, 0.2 μm, and 0.1 μm, 5 cycles per membrane, using the Lipex Biomembranes extruder, Model T001 (Vancouver, Canada). After, ammonium sulfate in the external medium was removed by ultracentrifugation (Ultracentrifuge Optima® L-80XP, Beckman Coulter, Brea, USA) at 150,000g, 4 °C, for 120 min. The pellet was resuspended with 0.9% (w/v) NaCl solution. Afterward, 10 mg/mL solution of IRN was incubated with SpHL or SpHL-Fol dispersion during 2 h at 4 °C. The non-encapsulated IRN was removed by ultracentrifugation using the same method described above.

#### 2.2.2. Liposomes physicochemical characterization

*2.2.2.1. Size distribution, zeta potential and encapsulation efficiency (% EE).* The mean diameter of liposomes was determined by dynamic light scattering at 25 °C at an angle of 90°. The zeta potential was evaluated by electrophoretic mobility determination at an angle of 90°. Size and zeta potential measurements were performed in triplicate using the nano ZS90 Zetasizer equipment (Malvern Instruments, England). The samples were diluted using a 0.9% (w/v) NaCl solution. The encapsulation efficiency (EE) of IRN in liposomes was determined by HPLC, using phosphate buffer: acenonitrile (70:30 v/v) + 0.2% triethylamine (pH 2.5, adjusted with phosphoric acid) as the mobile phase, and a reversed-phase C18 column with fluorescence detection [30].

*2.2.2.2. Nanoparticle tracking analysis.* The measurements were

performed using the Nanosight NS300 equipment (Malvern Instruments, England). The samples were prepared after dilution in ultrapure water (same external phase as the formulations) and introduced into the Nanosight sample chamber with a disposable syringe. The samples were measured at room temperature for 60 s with automatic detection. The suspension was irradiated by a laser source and light scattering. Images were captured by a charge-coupled device camera.

*2.2.3. pH-sensitive drug release study*

Drug release was carried out through dialysis with cellulose membranes (MWCO12000 Da) in HEPES-saline buffer at two different pHs (pH 5 and 7.4). Dialysis bags containing 500 μL of SpHL-IRN or free drug were added to vials containing 50 mL of the buffer and kept under agitation at 37 °C. At 30 min, 1, 2, 4, 8, and 24 h, aliquots of 1 mL of the buffer were collected and the same volume was replaced so that the concentration of the solution did not vary the amount of drug released was then calculated by HPLC.

*2.2.4. Confocal microscopy*

CT26 murine colon cancer tumor cells were seeded in 6-well plates with sterile coverslips ($2.5 \times 10^5$ cells/well) at 24 h before treatment. Cells were exposed to a solution of IRN, SpHL-IRN, or SpHL-IRN-Fol, at a drug concentration of 5 μM, for 12 h. After washing with PBS, cells were fixed with 3.7% (v/v) formaldehyde solution, slides were assembled using Prolong Gold Antifade Reagent (Thermo Fisher Scientific - Waltham, USA). Cells were analyzed in "Centro de Aquisição e Processamento de Imagens da UFMG (CAPI/UFMG)" using the LSM 880 microscope with Airyscan detector (ZEISS - Oberkochen, Germany). For image acquisition, a 63x objective lens and a Diode 370 nm (excitation of IRN) laser were used. The images were processed using the ZEN Blue Edition software version 2.3 lite (ZEISS -Oberkochen, Germany).

*2.2.5. In vivo studies*

*2.2.5.1. Cell culture.* CT26 cells were grown in RPMI-1640 medium (Gibco, USA), supplemented by 10% (v/v) fetal bovine serum, penicillin (100 IU/mL) and streptomycin (100 mg/mL). Cells were kept in humidified air (95%) containing 5% $CO_2$ at 37 °C. After 3–5 days of culture the cells were trypsinized and cell viability was assessed after staining with Trypan Blue. After centrifugation (5 min at 330 g), cells were resuspended in culture medium for inoculation into the BALB/c mice.

*2.2.5.2. Tumor inoculation.* Aliquots (100 μL) with $1.0 \times 10^6$ of CT26 cells were subcutaneously injected into the right flank of female BALB/c mice. Tumor cells were allowed to grow in vivo for 10 days until tumors reached, approximately, 100 $mm^3$.

*2.2.5.3. Antitumor activity.* After tumor development, mice were randomly split into 4 groups (n = 6 for each group): saline (control group); free IRN; SpHL-IRN; and SpHL-IRN-FOL. The total dose of IRN in all treatment groups was 120 mg/kg, divided into 4 administrations (30 mg/kg), every 2 days. Throughout the study, mice were weighed, and tumors were measured with caliper every 2 days, until the end of the experiment (Day 8) when mice were sacrificed. Tumor volumes were calculated from the formula:

$$V = (d_1)^2 \times d_2 \times 0.5$$

Where $d_1$ and $d_2$, represent the smallest and largest diameter, respectively. The inhibition ratio IR) was calculated on day 8 ($D_8$), as follows:

IR = 1 - (Mean RTV of drug-treated group/Mean RTV of control group) × 100.

Where, RTV = Tumor volume $D_8$/Tumor volume $D_0$.

*2.2.5.4. Hematological and biochemical study.* At the end of the study, the animals were euthanized immediately after whole blood was collected by puncture of the brachial plexus into tubes containing anticoagulant (EDTA). The hematological parameters evaluated included hemoglobin, number of red blood cells, hematocrit, hematimetric indices, red blood cell distribution width (RDW), global and differential leukocyte count and number of platelets, as described in our laboratory previously [31].

Plasma was obtained through centrifugation (3000 rpm, 15 min) and biochemical parameters were quantified. Renal function was evaluated through blood urea nitrogen and creatinine parameters and liver function through amino transferase (ALT) and aspartate amino transferase (AST) analysis [32].

*2.2.5.5. Histological analysis.* At the end of the study, the main organs (primary tumor, lungs, large intestine, liver and kidneys) were excised, embedded in paraffin and submitted to hematoxylin-eosin (H&E) staining for toxicity analysis [32].

*2.2.6. Statistical analysis*

All data are expressed as mean ± SD. Means among the various groups were compared by an analysis of variance (ANOVA), followed by Tukey's test (GraphPad PRISM, version 6.0). A *P*-value of $< 0.05$ was considered be statistically significant.

## 3. Results

*3.1. Size distribution, zeta potential and encapsulation efficiency (% EE)*

The mean diameter, polydispersity index, zeta potential, % EE, and the drug loading of the liposomal formulations are described in Table 1.

Liposomes were homogeneous (low PDI) with a diameter smaller than 200 nm. The zeta potential was close to neutrality for all formulations, which can be beneficial for its pharmacokinetic properties [33]. DLS results were further validated by nanoparticulate tracking studies (Fig. S1), in which a monodispersed population was found with the majority (90%) of particles having 155 nm in diameter.

*3.2. pH-sensitive drug release studies*

*In vitro* pH sensitivity was evaluated for SpHL-IRN and free IRN at different pHs (7.4 and 5.0) and the results are shown in Fig. 1.

*In vitro* pH-sensitivity of SpHL-IRN was evaluated as a function of time at different pHs (7.4 and 5.0), Fig. 1**.** No statistical changes were observed with free drug. However, the IRN encapsulated in liposomes presented a pH and time- dependent release demonstrating a greater stability and retention capability of the nanoparticle [34]. As seen in Fig. 1, up to the 30 min timepoint, the release pattern of IRN encapsulated in SpHL is similar at both pHs. However, at timepoints of 1, 2 and

**Table 1**
Physicochemical characterization of SpHL, SpHL-Fol, SpHL-IRN and SpHLIRN-Fol.

| Formulation | Mean Diameter (nm) | PDI | Zeta potential (mV) | % EE | Drug loading (mg/mL) |
|---|---|---|---|---|---|
| **SpHL-blank** | 159.2 ± 3.9 | 0.09 ± 0.03 | - 4.1 ± 0.6 | – | – |
| **SpHL-fol-blank** | 160.1 ± 4.0 | 0.09 ± 0.03 | - 4.1 ± 0.6 | – | – |
| **SpHL-IRN** | 169.0 ± 6.0 | 0.12 ± 0.05 | -11.1 ± 0.8 | 66.2 ± 3.0 | 6.6 ± 0.3 |
| **SpHL-FOL-IRN** | 165.2 ± 3.1 | 0.12 ± 0.08 | -9.10 ± 1.2 | 62.3 ± 0.9 | 6.2. ± 0.1 |

***Note*:** Data are expressed by the mean (n = 3) ± S.D. of the mean. All data were analyzed by one-way ANOVA analysis of variance followed by Tukey's post-test ($P > 0.05$).

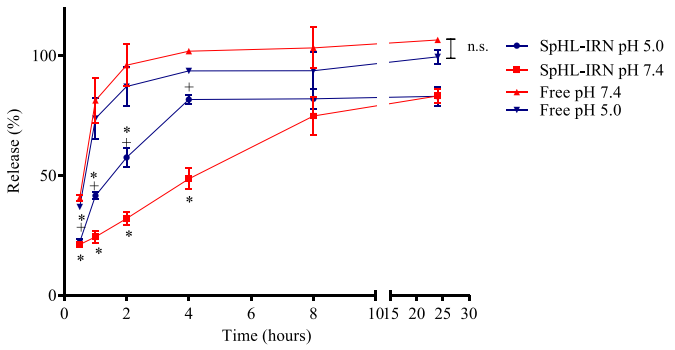


**Fig. 1. pH dependent release of IRN.** The percent release profile of SpHL-IRN at pH 7.4 (red lines) and pH 5.0 (blue lines) is shown over 24 h. ***Note:*** *P < 0.05 as compared with free-IRN (pH 5 and pH 7); +P < 0.05 between the SpHL-IRN pH 7.4. Data are expressed by the mean (n = 3) ± S.D. of the mean. All data were analyzed by one-way ANOVA analysis of variance followed by Tukey's post-test. (For interpretation of the references to colour in this figure legend, the reader is referred to the web version of this article.)

4 h a more pronounced release of the drug is found at pH 5 when compared to pH 7.4 ($p < 0.05$), which corroborates the hypothesis that a pH reduction promotes a destabilization of the nanosystem, culminating in greater drug release. These finding confirm the pH sensitivity for SpHL, which might be beneficial for the drug delivery in the tumor microenvironment [16].

### 3.3. Confocal microscopy

To validate drug release and uptake in colon cancer cells we performed confocal microscopy, Fig. 2. IRN was visualized intracellularly, localized mostly in the cytoplasmatic and peri-nuclear regions. A small uptake in the nuclei can be observed for all groups (Free IRN, SpHL-IRN, SpHL-IRN-Fol) investigated. These results suggest the efficient IRN delivery inside the cell for all formulations at the evaluated time [35].

### 3.4. Anti-tumor activity

The antitumor activity of free-IRN and liposomal preparations (SpHL-IRN and SpHLIRN-Fol) were evaluated in CT26 tumor-bearing BALB/c mice. Tumor volume growth curves (Fig. 3**A**) had drastically different profiles among the groups. Animals that received liposomal formulations had significantly smaller tumor volumes when compared to control groups (saline and free IRN groups), $p < 0.05$. In addition, the animals that received liposomal formulation functionalized with folate (SpHLIRN-Fol) had significantly smaller tumor volumes than any other group, including non-functionalized SpHL-IRN. These data support that folate was advantageous in tumor targeting and anti-tumor activity. Fig. 3**B** shows the tumor volumes at the end of the experiment for all the groups, confirming the higher efficiency of SpHL-IRN-Fol in controlling tumor growth.

The tumor volume inhibition ratio (TV-IR), shown in Table 2, corroborates the data presented in tumor growth curves. Overall, liposomal formulations were more effective at inhibiting tumor growth than free IRN or saline. Treatment with SpHL-IRN-Fol resulted in an even more extensive tumor growth inhibition when compared to SpHL-IRN (57.8% and 41.5%, respectively).

### 3.5. Hematological and biochemical study

Hematological parameters of control and mice treated with Free-IRN, SpHL-IRN and SpHL-IRN-Fol are shown in Table 3. RBC and platelets counts, HGB concentrations, and HCT values were similar in all groups and presented no significant difference ($p > 0.05$) when compared to those of the control group. In addition, there was no change in the leukocyte series for all groups.

Biochemical parameters indicative of renal (blood urea nitrogen and serum creatinine) and hepatic (ALT and AST) toxicity did not show significant changes among groups. These results are consistent with the lack of histological alteration that was observed in the renal and hepatic tissue of the mice treated with different formulations containing IRN, which confirms that the treatment at the doses used, as expected, did not cause high toxicity (Fig. 4**A–D**). Additionally, body weight measurements were taken to evaluate overall toxicity of administered formulations. No significant body weight changes were found after therapeutic administration in any of the groups investigated ($p > 0.05$) (Fig. 4**E**).

### 3.6. Histological analysis

Both tumor and normal tissues were evaluated by histology for necrosis and metastasis. Histological analysis of colorectal cancer tumors is presented in Fig. 5. Treatment with free IRN, SpHL-IRN or SpHL-IRN-Fol, showed extensive necrosis due to IRN-induced cell death (Fig. 5**F**; 5**G** and 5**H**, respectively). Liver and large intestine tissues were evaluated for the appearance of metastases (Fig. 6) however no metastatic foci were found in the tissues evaluated.

## 4. Discussion

Conventional systemic therapies for the treatment of cancer consist mostly of antineoplastic drugs that, in general, have low specificity and high toxicity, which limits the either the dose that can be administered or the number of cycles a patient can undergo. In the last few decades, with new understandings of the molecular characteristics of tumors and its microenvironment, anticancer therapy research focus has shifted to include more specialized and targeted approaches [36,37]. Among these strategies, the use of nanostructured drug delivery systems has had a profound impact on cancer therapeutics research. A wide range of nanomaterials have emerged as alternative tools that can deliver

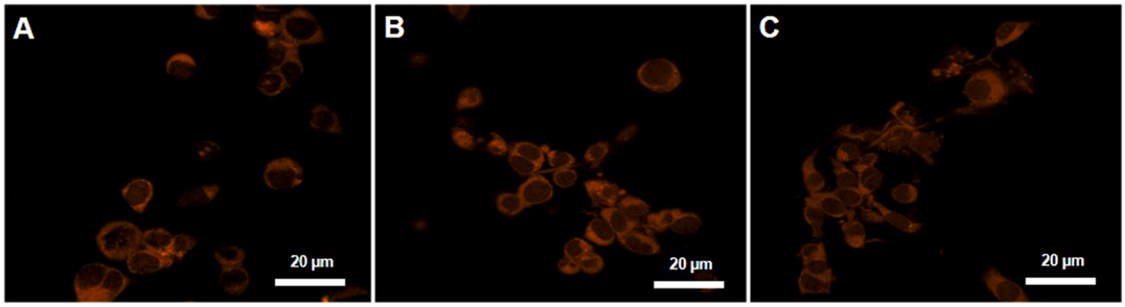


**Fig. 2. Liposomal encapsulated IRN is efficiently taken up in colon cancer cells.** Confocal microscopy images of CT26 murine colon cancer tumor cells after 24 h-incubation with A = free IRN, B = SpHL-IRN or C = SpHLIRN-Fol treatments (IRN concentration 5 µM). Amplification of 63 ×. Diode 370 nm (excitation of IRN).

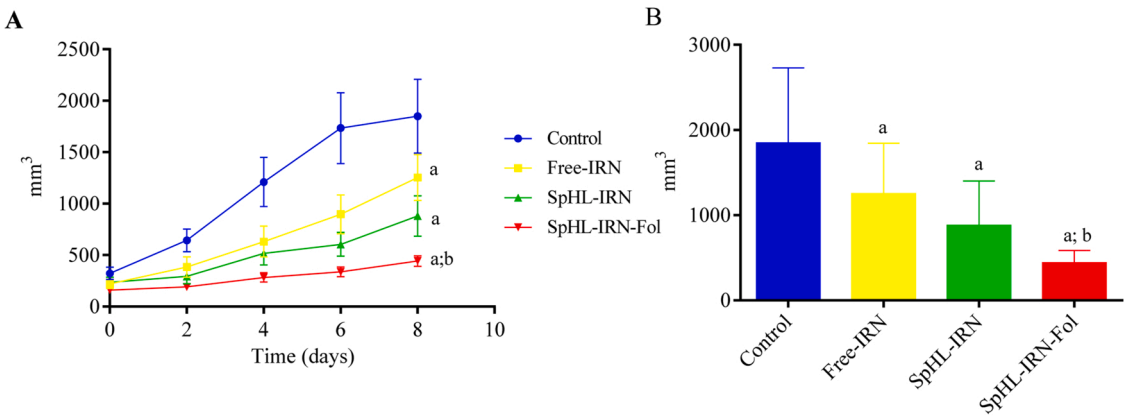


**Fig. 3. Liposomes containing IRN are more effective than free drug.** (**A**) Antitumor effect of SpHL (control group), IRN, SpHL-IRN, and SpHL-IRN-Fol on the growth of CT26 colon tumor-bearing female BALB/c mice. Each treatment was intravenously administered 3 times, every 2 days, at dose of 30 mg/kg. (**B**) Volume tumoral at the end of the experiments, day 8, after treatments. ***Note*:** Data are expressed by the mean ± standard deviation of the mean (n = 6). Growth curves were analyzed by regression. a Represents statistical differences ($P < 0.05$) as compared with control group. b Represents statistical differences ($P < 0.05$) as compared with free-IRN. All data were analyzed by one-way ANOVA analysis of variance followed by Tukey's post-test.

**Table 2**
Relative tumor volume (RTV) and tumor growth inhibition ratio (IR) after administration of free-IRN, SpHL-IRN and SpHL-IRN-Fol.

| Treatment group | RTV | IR (%) |
|---|---|---|
| **Free-IRN** | 5,9 ± 3,21 | 16,6 |
| **SpHL-IRN** | 4,1 ± 1,43 | 41,5 |
| **SpHL-IRN-Fol** | 2,9 ± 1,42[a] | 57,8 |

***Note*:** [a]Represents significant difference as compared with the Free-IRN P-values less than 0.05; the data were analyzed by one-way ANOVA analysis of variance followed by Tukey's test. Data expressed as mean ± S.D. of the mean (n = 6).

**Table 3**
Hematological parameters of control mice treated with 3 doses of IRN formulations.

| Parameters | Treatments | | | |
|---|---|---|---|---|
| | CTL | IRN | SPHL-IRN | SPHL-IRN-Fol |
| RBC (cell/mm$^3$ x 10$^6$) | 4,9 ± 2,2 | 5,3 ± 1,0 | 5,7 ± 0,9 | 5,9 ± 0,5 |
| Hemoglobin (g/L) | 9,0 ± 4,7 | 8,3 ± 2,6 | 10,3 ± 2,2 | 11,0 ± 1,4 |
| HCT (%) | 25,1 ± 10,6 | 27,4 ± 5,3 | 28,8 ± 4,6 | 30,3 ± 2,5 |
| WBC (cell/mm$^3$ x 10$^3$) | 6,5 ± 4,2 | 2,5 ± 1,0 | 3,1 ± 1,0 | 2,8 ± 1,0 |
| Granulocyte (cell/mm$^3$ x 10$^3$) | 2,9 ± 1,9 | 1,2 ± 0,5 | 1,4 ± 0,5 | 1,2 ± 0,5 |
| Not granulocyte (cell/mm$^3$ x 10$^3$) | 3,56 ± 2,3 | 1,3 ± 0,6 | 1,7 ± 0,6 | 1,5 ± 0,5 |
| RDW (%) | 14,9 ± 1,6 | 16,2 ± 1,3 | 16,1 ± 0,4 | 15,8 ± 1,0 |
| PLT (cell/mm$^3$ x 10$^3$) | 261,2 ± 157,0 | 211,3 ± 78,5 | 276,4 ± 55,9 | 233,5 ± 78,3 |

***Note*:** Evaluation of the hematological parameters was carried out 10 days after treatment of mice with the IRN formulations. Results were expressed as the mean ± standard deviation. Abbreviations: HGB (hemoglobin), RBC (red blood cells), HTC (hematocrit), PLT (platelets), WBC (total white blood cells). Data expressed as mean ± S.D. of the mean (n = 6). All data were analyzed by one-way ANOVA analysis of variance followed by Tukey's post-test ($P > 0.05$)

otherwise toxic chemotherapeutics to tumor sites with improved therapeutic efficacy. Among the available versatile materials, liposomes have been extensively employed as smart carriers able to modify biodistribution, metabolism, and in vivo elimination of drugs [16,38–40].

It is well known that antitumor activity is directly proportional to the intracellular concentration of the active drugs/metabolites [16,21] and its toxicity is correlated with the amount of drug distributed to off-target tissues. Thus, an ideal drug carrier should be specifically taken up by the tumor and allow internalization of the drug into tumor cells while reducing drug uptake by healthy tissue. The ability to design liposomes to both be pH sensitive and promote active tumor targeting makes it an attractive candidate as a drug nanocarrier. The pH responsiveness of liposomes may be attributed to the presence of dioleoylphosphatidylethanolamine (DOPE) in the liposome bilayer. Since DOPE by itself is uncapable of forming a lamellar structure, the use of stabilizing agents such as cholesteryl hemisuccinate (CHEMS) is required for a liposome structure formation. At physiological pH, CHEMS is ionized and inserted between the DOPE molecules resulting in electrostatic repulsions between the CHEMS ionized carboxyl groups and DOPE phosphate groups, resulting in the formation of a liposomal bilayer. In contrast, at a lower pH, CHEMS is protonated promoting destabilization of the liposomal structure and consequently drug release. Since the tumor microenvironment is more acidic than surrounding healthy tissue, a targeted and optimized drug released is obtained resulting in optimized chemotherapeutic drug action [11,16,41,42]. In addition to their optimal fusogenic properties, the inclusion of targeting moieties on the liposomal surface, such as folic acid, can lead to increased tumor targeting capabilities and chemotherapeutic efficacy [27]. With all that in mind, we have constructed pH-sensitive liposomes with tumor targeting capabilities, encapsulated with a chemotherapeutic drug IRN, for improved therapeutic response in colorectal cancer.

In the present study, the liposomes (SpHL-IRN-Fol and SpHL-IRN) were successfully synthesized with similar and monodisperse vesicle diameter in all formulations. Liposomes were obtained with a diameter of less than 200 nm, which allows its extravasation to the tumor tissue by EPR effect [43]. SpHL-IRN-Fol and SpHL-IRN presented slightly negative zeta potential due to the presence of phosphate groups of the phospholipids in the liposome composition. However, the presence of PEG chains on the surface of the liposome produces a hydrophilic layer and reduces its electrophoretic mobility resulting in a zeta potential close to neutrality [40]. This is important because, once in the blood stream, conventional nanoparticles and negatively charged particles can be opsonized and massively cleared by phagocytosis by immune cells and removed from systemic circulation, and consequently, avoid the effective delivery of the nano drug to organs [44].

Cytotoxic drugs encapsulated in liposomes are normally unable to act on their therapeutic targets or cause toxicity until they are released from the confines of the carrier, and thus liposomal drug delivery can

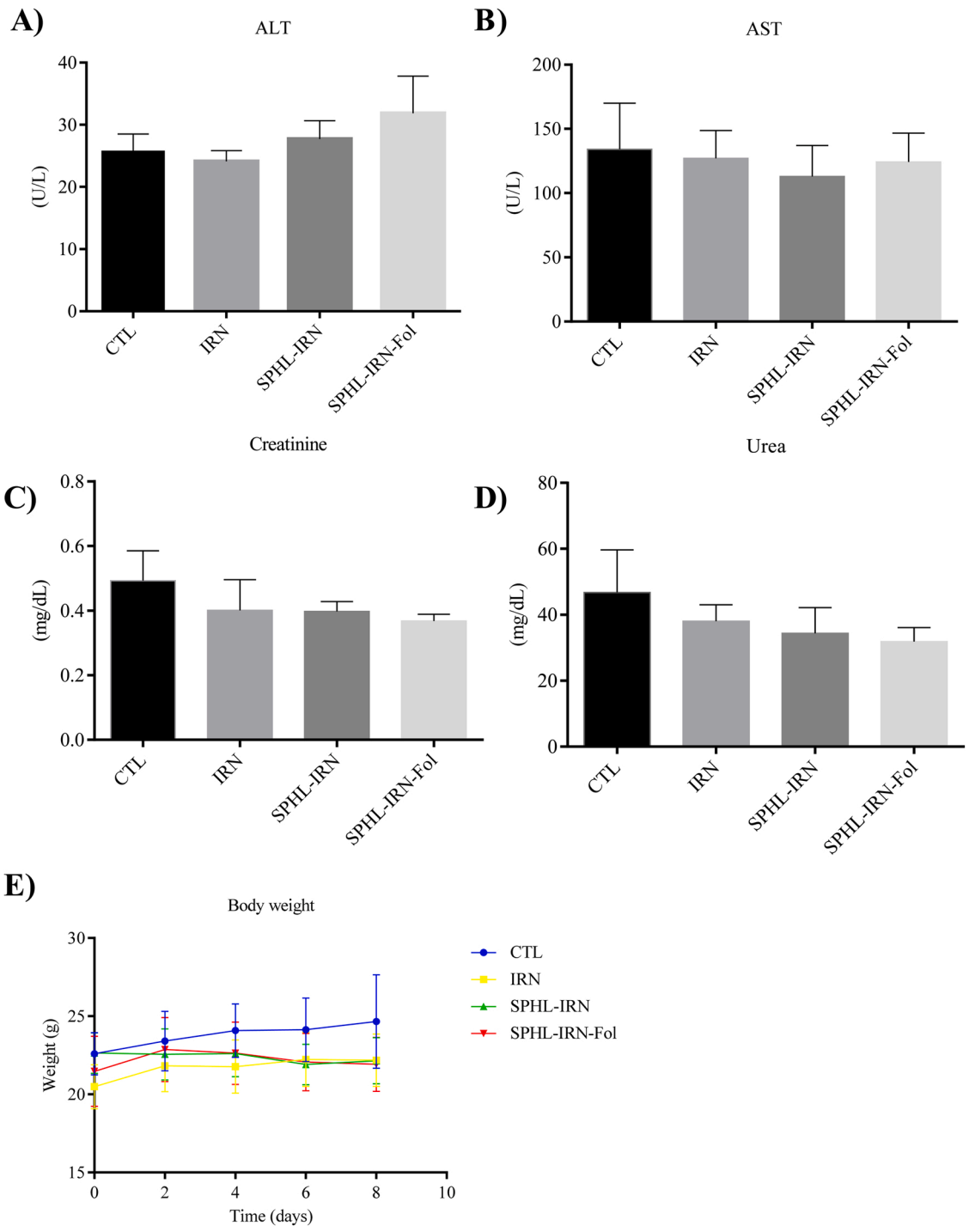


**Fig. 4. Evaluation of kidneys and liver toxicity.** Biochemical parameters of control mice treated with 3 doses of IRN formulations were evaluated for kidneys toxicity (A and B), liver toxicity (C and D) and body weight (E). Data expressed as mean ± S.D. of the mean (n = 6). ***Note*:** Evaluation of the biochemical parameters was carried out 10 days after treatment of mice with the IRN formulations. Results were expressed as the mean ± standard deviation. Abbreviations: ALT (alanine aminotransferase), and AST (aspartate aminotransferase). All data were analyzed by one-way ANOVA analysis of variance followed by Tukey's post-test ($P > 0.05$).

itself be regarded as a prodrug strategy [34]. Although local activation of IRN to SN-38 has yet to be shown, carboxylesterases have a widespread distribution in different tumor types and are active in macrophages, where liposomes are primarily captured [45–47]. Thus, the ability of liposomal-mediated drug release at the desired tissue is extremely important. The pH-sensitive liposomes showed a greater release of liposomal content in acidic pH when compared to physiological pH. This is advantageous to achieve optimal balance between tumor uptake and protection of off-target tissue, especially when the encapsulated drug is considered a prodrug. pH sensitivity allowed IRN to be released only after it reached tumor sites where it can be activated locally [48].

Since IRN is a prodrug and is usually activated once inside the cells, its internalization is extremely important. However, only a few studies have reported the subcellular localization of camptothecin derivatives and the published results are somewhat heterogeneous [35]. Herein, confocal microscopy images demonstrated the presence of IRN in the intracellular environment in all groups evaluated, which confirms that

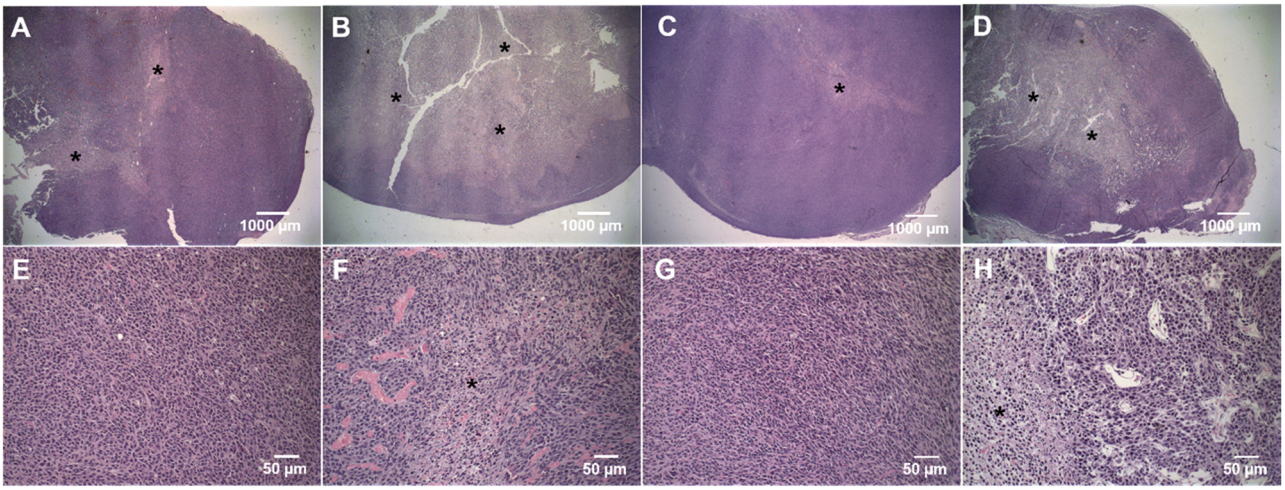


**Fig. 5. Histopathological analysis of tumor necrosis.** Histological sections of primary tumor from CT26 colorectal tumor-bearing female BALB/c mice treated with free IRN, SpHL-IRN or SpHL-IRN-Fol stained by hematoxylin & eosin. (**A**) control group at amplification of 2x. (**B**) Free-IRN-treated at amplification of 2x. (**C**) SpHL-IRN-treated at amplification of 2x. (**D**) SpHL-IRN-Fol-treated at amplification of 2x. (**E**) control group at amplification of 20x. (**F**) Free-IRN-treated at amplification of 20x. (**G**) SpHL-IRN-treated at amplification of 20x. (**H**) SpHL-IRN-Fol-treated at amplification of 20x. The black asterisks indicate areas of tumor necrosis.

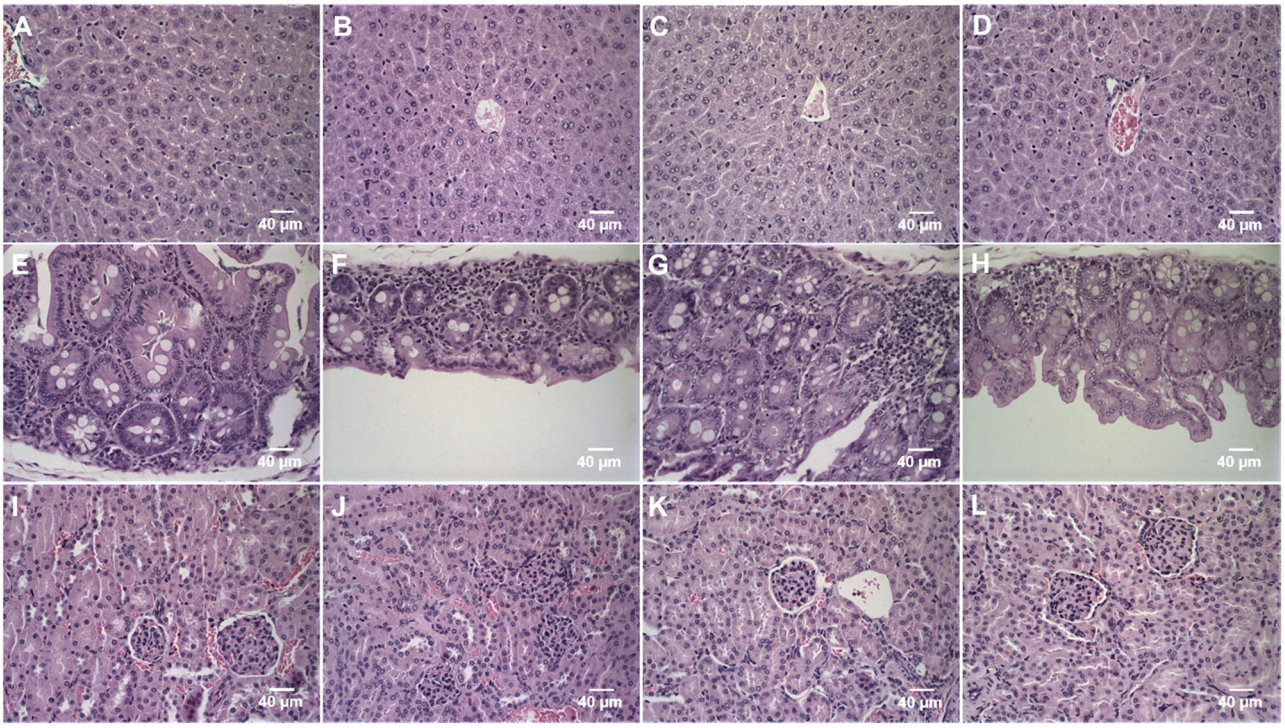


**Fig. 6. Histopathological analysis of liver and intestinal toxicity.** Histological sections of tissues from CT26 colorectal tumor-bearing female BALB/c mice treated with free IRN, SpHL-IRN or SpHL-IRN-Fol stained by hematoxylin & eosin. (**A**) control group liver. (**B**) Fre-IRN-treated liver. (**C**) SpHL-IRN-treated liver. (**D**) SpHL-IRN-Fol-treated liver. (**E**) control group large intestine. (**F**) Free-IRN-treated large intestine. (**G**) SpHL-IRN-treated large intestine. (**H**) SpHL-IRN-Fol-treated large intestine. (**I**) control group kidney. (**J**) Free-IRN-treated kidney. (**K**) SpHL-IRN-treated kidney. (**L**) SpHL-IRN-Fol-treated kidney. Amplification of 40x.

encapsulation into liposomal formulations did not compromise the capacity of IRN to be internalized by tumor cells.

The CT26 colorectal tumor-bearing BALB/c mouse model is a commonly used experimental animal model to study angiogenesis and antitumor activity of several pharmaceutical formulations [49]. Heterotopic implantation models such as subcutaneous tumor implants in mice have been traditionally used to evaluate antitumor treatment because of their reproducibility and monitoring of tumor formation [49, 50]. Our results demonstrated fast tumor growth in the control group. Even though IRN treatment is potentially highly active against CT26 colorectal tumor cells in vivo, a very high tumor growth rate was still observed in animals that received free IRN [51]. However, drug encapsulation in liposomes enhanced its antitumor activity. More importantly, active targeting of liposomes with the presence of acid folate contributed positively for anti-tumor effects. Significantly lower tumor volumes were found for animals administered with SpHL-IRN-Fol when compared to all other groups investigated. That group had the highest inhibition rate (57.8%), which had around 3.4 times higher

anti-tumor efficiency than the free drug. Comparable tumor growth inhibition was previously reported to folate-coated liposomes highlighting the efficiency of using folate-targeting [52]. Histological analysis of tumor tissue presented similar morphological characteristics among groups with central areas of necrosis and proliferation of pleomorphic cells at the periphery infiltrated by leukocytes (Fig. 4) [25]. However, the histological analysis of the primary tumor showed greater necrosis areas in the SpHL-IRN-Fol treated group when compared to all other groups investigated. These data make it clear that not only drug encapsulation but also pH sensitiveness and active targeting the greatly enhanced the antitumor activity. In fact, some studies have shown that folate-targeted liposomes had a potential role in overcoming drug resistance because of the bypass of the P-glycoprotein efflux pump [53, 54]. Gabizon et al. also described that FR-targeted liposomal delivery could reverse multidrug resistance to doxorubicin [53]. Since heterotopic tumor models lack fully developed tumor microenvironments, further studies in more clinically relevant tumor models such as orthotopic models are necessary for better assessment of positive impact of active targeting in anti-tumor efficacy.

Noteworthy, no apparent systemic toxicity was found in any of the groups investigated. Body weight measurements as well as hematological and biochemical tests (hepatic and renal) revealed no acute toxicity to liposome formulations. Altogether, our results indicate the potential of our formulated IRN encapsulated liposome as an alternative drug delivery system for colorectal cancer [55,56].

## 5. Conclusion

In this study, we developed and characterized a folate-coated and pH-sensitive liposome drug delivery system containing irinotecan (SpHL-IRN-Fol) for the treatment of colorectal cancer. This novel multifunctional formulation demonstrated to have significantly improved antitumor activity than IRN alone with no evidence of toxicity. These data support further preclinical development of SpHL-IRN-Fol as a promising drug delivery system for the treatment of colorectal cancer.

## CRediT authorship contribution statement

**Shirleide Santos Nunes:** Conceptualization, Methodology, Formal analysis, Investigation, Writing – original draft; **Sued Eustaquio Mendes Miranda:** Formal analysis, Investigation; **Juliana de Oliveira Silva:** Formal analysis, Investigation; **Renata Salgado Fernandes:** Formal analysis, Investigation; **Janaína de Alcântara Lemos:** Formal analysis, Investigation; **Carolina de Aguiar Ferreira:** Formal analysis, Writing – review & editing; **Danyelle M. Townsend:** Writing – review & editing; **Geovanni Dantas Cassali:** Formal analysis, Visualization: **Mônica Cristina Oliveira:** Conceptualization, Methodology, Resources, Writing – review & editing; **André Luís Branco de Barros:** Conceptualization, Methodology, Resources, Supervision, Writing – review & editing.

## Conflict of interest statement

The authors declare they have no conflict of interest.

## Acknowledgments

The authors would like to thank Fundação de Amparo à Pesquisa do Estado de Minas Gerais (FAPEMIG-Brazil), Conselho Nacional de Desenvolvimento Científico e tecnológico (CNPq-Brazil) for their financial support and scholarship. The authors also thank the “Centro de Aquisição e Processamento de Imagens da UFMG (CAPI/UFMG)” for the assistance with confocal images. DMT is supported by the NCRR P20RR024485 in the Analytical Redox Biochemistry Core Facility at MUSC.

## Appendix A. Supporting information

Supplementary data associated with this article can be found in the online version at doi:10.1016/j.biopha.2021.112317.

## References

[1] H. Wei, J. Song, H. Li, Y. Li, S. Zhu, X. Zhou, X. Zhang, L. Yang, ScienceDirect Active loading liposomal irinotecan hydrochloride: preparation, in vitro and in vivo evaluation, Asian J. Pharm. Sci. 8 (2013) 303–311, https://doi.org/10.1016/j.ajps.2013.10.006.

[2] P. Piedbois, Efficacy of intravenous continuous infusion of fluorouracil compared with bolus administration in advanced colorectal cancer, J. Clin. Oncol. 16 (1998) 301–308, https://doi.org/10.1200/JCO.1998.16.1.301.

[3] W.J.M. Jansen, B. Zwart, S.T.M. Hulscher, G. Giaccone, H.M. Pinedo, E. Boven, CPT-11 in human colon-cancer cell lines and xenograft: characterization of cellular sensitivity determinants, Int. J. Cancer 70 (1997) 335–340, https://doi.org/10.1002/(SICI)1097-0215(19970127)70:3<335::AID-IJC15>3.0.CO;2-E.

[4] A. Casadó, M.L. Sagristá, M. Mora, A novel microfluidic liposomal formulation for the delivery of the SN-38 camptothecin: characterization and in vitro assessment of its cytotoxic effect on two tumor cell lines, Int. J. Nanomed. 13 (2018) 5301–5320, https://doi.org/10.2147/IJN.S166219.

[5] J.I. Hare, R.W. Neijzen, M. Anantha, N. Dos Santos, N. Harasym, M.S. Webb, T. M. Allen, M.B. Bally, D.N. Waterhouse, Treatment of colorectal cancer using a combination of liposomal irinotecan (Irinophore CTM) and 5-fluorouracil, PLoS One 8 (2013), e62349, https://doi.org/10.1371/journal.pone.0062349.

[6] R. Garcia-Carbonero, J.G. Supko, Current perspectives on the clinical experience, pharmacology, and continued development of the camptothecins, Clin. Cancer Res. 8 (2002) 641–661.

[7] S. Chen, M.F. Yueh, C. Bigo, O. Barbier, K. Wang, M. Karin, N. Nguyen, R.H. Tukey, Intestinal glucuronidation protects against chemotherapy-induced toxicity by irinotecan (CPT-11), Proc. Natl. Acad. Sci. U. S. A. 110 (2013) 19143–19148, https://doi.org/10.1073/pnas.1319123110.

[8] E. Raymond, V. Boige, S. Faivre, G.J. Sanderink, O. Rixe, L. Vernillet, C. Jacques, M. Gatineau, M. Ducreux, J.P. Armand, Dosage adjustment and pharmacokinetic profile of irinotecan in cancer patients with hepatic dysfunction, J. Clin. Oncol. 20 (2002) 4303–4312, https://doi.org/10.1200/JCO.2002.03.123.

[9] C.H. Takimoto, J. Wright, S.G. Arbuck, Clinical applications of the camptothecins, Biochim. Biophys. Acta Gene Struct. Expr. 1400 (1998) 107–119, https://doi.org/10.1016/S0167-4781(98)00130-4.

[10] Q. Du, X. Qin, M. Zhang, Z. Zhao, Q. Li, X. Ren, A mitochondrial-metabolism-regulatable carrier-free nanodrug to amplify the sensitivity of photothermal therapy, ChemComm 57 (2021) 8993–8996, https://doi.org/10.1039/d1cc02755g.

[11] T.M. Allen, P.R. Cullis, Liposomal drug delivery systems: from concept to clinical applications, Adv. Drug Deliv. Rev. 65 (2013) 36–48, https://doi.org/10.1016/j.addr.2012.09.037.

[12] J.C. Kraft, J.P. Freeling, Z. Wang, R.J.Y. Ho, Emerging research and clinical development trends of liposome and lipid nanoparticle drug delivery systems, J. Pharm. Sci. 103 (2014) 29–52, https://doi.org/10.1002/jps.23773.

[13] J.Y. Choi, T. Ramasamy, T.H. Tran, S.K. Ku, B.S. Shin, H.G. Choi, C.S. Yong, J. O. Kim, Systemic delivery of axitinib with nanohybrid liposomal nanoparticles inhibits hypoxic tumor growth, J. Mater. Chem. B 3 (2015) 408–416, https://doi.org/10.1039/c4tb01442a.

[14] C.M. Dawidczyk, C. Kim, J.H. Park, L.M. Russell, K.H. Lee, M.G. Pomper, P. C. Searson, State-of-the-art in design rules for drug delivery platforms: lessons learned from FDA-approved nanomedicines, J. Control. Release 187 (2014) 133–144, https://doi.org/10.1016/j.jconrel.2014.05.036.

[15] M.A. Madni, M. Sarfraz, M. Rehman, M. Ahmad, N. Akhtar, S. Ahmad, N. Tahir, S. Ijaz, R. Al-Kassas, R. Löbenberg, Liposomal drug delivery: a versatile platform for challenging clinical applications, J. Pharm. Pharm. Sci. 17 (2014) 401–426, https://doi.org/10.18433/j3cp55.

[16] J.O. Silva, R.S. Fernandes, S.C.A. Lopes, V.N. Cardoso, E.A. Leite, G.D. Cassali, M. C. Marzola, D. Rubello, M.C. Oliveira, A.L.B. de Barros, pH-sensitive, long-circulating liposomes as an alternative tool to deliver doxorubicin into tumors: a feasibility animal study, Mol. Imaging Biol. 18 (2016) 898–904, https://doi.org/10.1007/s11307-016-0964-7.

[17] F.N. Carlesso, R.S. Araújo, L.L. Fuscaldi, S.E.M. Miranda, D. Rubello, C.S. Teixeira, D.C. Dos Reis, E.A. Leite, J.N. Silveira, S.O.A. Fernandes, G.D. Cassali, M.C. De Oliveira, P.M. Colletti, A.L.B. De Barros, V.N. Cardoso, Preliminary data of the antipancreatic tumor efficacy and toxicity of long-circula ting and pH-sensi tive liposomes containing cisplatin, Nucl. Med. Commun. 37 (2016) 727–734, https://doi.org/10.1097/MNM.0000000000000505.

[18] M.S. Franco, C.A. Silva, E.A. Leite, J.N. Silveira, C.S. Teixeira, V.N. Cardoso, E. Ferreira, G.D. Cassali, A.L. Branco de Barros, M.C. Oliveira, Investigation of the antitumor activity and toxicity of cisplatin loaded pH-sensitive-pegylated liposomes in a triple negative breast cancer animal model, J. Drug Deliv. Sci. Technol. 62 (2021), 102400, https://doi.org/10.1016/j.jddst.2021.102400.

[19] M.S. Franco, M.C. Roque, A.L.B. de Barros, J. de Oliveira Silva, G.D. Cassali, M. C. Oliveira, Investigation of the antitumor activity and toxicity of long-circulating and fusogenic liposomes co-encapsulating paclitaxel and doxorubicin in a murine breast cancer animal model, Biomed. Pharmacother. 109 (2019) 1728–1739, https://doi.org/10.1016/j.biopha.2018.11.011.

[20] S.B. dos Reis, J. de Oliveira Silva, F. Garcia-Fossa, E.A. Leite, A. Malachias, G. Pound-Lana, V.C.F. Mosqueira, M.C. Oliveira, A.L.B. de Barros, M.B. de Jesus, Mechanistic insights into the intracellular release of doxorubicin from pH-sensitive liposomes, Biomed. Pharmacother. 134 (2021), 110952, https://doi.org/10.1016/j.biopha.2020.110952.

[21] M.C. De Oliveira, V. Rosilio, P. Lesieur, C. Bourgaux, P. Couvreur, M. Ollivon, C. Dubernet, pH-sensitive liposomes as a carrier for oligonucleotides: a physico-chemical study of the interaction between DOPE and a 15-mer oligonucleotide in excess water, Biophys. Chem. 87 (2000) 127–137, https://doi.org/10.1016/S0301-4622(00)00180-0.

[22] L.O.F. Monteiro, R.S. Fernandes, L. Castro, D. Reis, G.D. Cassali, F. Evangelista, C. Loures, A.P. Sabino, V. Cardoso, M.C. Oliveira, A. Branco De Barros, E.A. Leite, Paclitaxel-loaded folate-coated pH-sensitive liposomes enhance cellular uptake and antitumor activity, Mol. Pharm. 16 (2019) 3477–3488, https://doi.org/10.1021/acs.molpharmaceut.9b00329.

[23] Y. Lu, P.S. Low, Folate-mediated delivery of macromolecular anticancer therapeutic agents, Adv. Drug Deliv. Rev. 54 (2002) 675–693, https://doi.org/10.1016/S0169-409X(02)00042-X.

[24] D.C.F. Soares, V.N. Cardoso, A.L.B. De Barros, C.M. De Souza, G.D. Cassali, M.C. De Oliveira, G.A. Ramaldes, Antitumoral activity and toxicity of PEG-coated and PEG-folate-coated pH-sensitive liposomes containing 159Gd-DTPA-BMA in Ehrlich tumor bearing mice, Eur. J. Pharm. Sci. 45 (2012) 58–64, https://doi.org/10.1016/j.ejps.2011.10.018.

[25] J. de Oliveira Silva, R.S. Fernandes, C.M. Ramos Oda, T.H. Ferreira, A.F. Machado Botelho, M. Martins Melo, M.C. de Miranda, D. Assis Gomes, G. Dantas Cassali, D. M. Townsend, D. Rubello, M.C. Oliveira, A.L.B. de Barros, Folate-coated, long-circulating and pH-sensitive liposomes enhance doxorubicin antitumor effect in a breast cancer animal model, Biomed. Pharmacother. 118 (2019), 109323, https://doi.org/10.1016/j.biopha.2019.109323.

[26] A.A. Lohade, R.R. Jain, K. Iyer, S.K. Roy, H.H. Shimpi, Y. Pawar, M.G.R. Rajan, M. D. Menon, A novel folate-targeted nanoliposomal system of doxorubicin for cancer targeting, AAPS PharmSciTech 17 (2016) 1298–1311, https://doi.org/10.1208/s12249-015-0462-2.

[27] Z.C. Soe, R.K. Thapa, W. Ou, M. Gautam, H.T. Nguyen, S.G. Jin, S.K. Ku, K.T. Oh, H.G. Choi, C.S. Yong, J.O. Kim, Folate receptor-mediated celastrol and irinotecan combination delivery using liposomes for effective chemotherapy, Colloids Surf. B Biointerfaces 170 (2018) 718–728, https://doi.org/10.1016/j.colsurfb.2018.07.013.

[28] A.D. Bangham, M.M. Standish, J.C. Watkins, Diffusion of univalent ions across the lamellae of swollen phospholipids, J. Mol. Biol. 13 (1965) 238–252, https://doi.org/10.1016/S0022-2836(65)80093-6.

[29] D. dos Santos Ferreira, B.L. Jesus de Oliveira Pinto, V. Kumar, V.N. Cardoso, S. O. Fernandes, C.M. Souza, G.D. Cassali, A. Moore, D.E. Sosnovik, C.T. Farrar, E. A. Leite, R.J. Alves, M.C. de Oliveira, A.R. Guimarães, P. Caravan, Evaluation of antitumor activity and cardiac toxicity of a bone-targeted ph-sensitive liposomal formulation in a bone metastasis tumor model in mice, Nanomed. Nanotechnol. Biol. Med. 13 (2017) 1693–1701, https://doi.org/10.1016/j.nano.2017.03.005.

[30] P.G. Tardi, R.C. Gallagher, S. Johnstone, N. Harasym, M. Webb, M.B. Bally, L. D. Mayer, Coencapsulation of irinotecan and floxuridine into low cholesterol-containing liposomes that coordinate drug release in vivo, Biochim. Biophys. Acta Biomembr. 1768 (2007) 678–687, https://doi.org/10.1016/j.bbamem.2006.11.014.

[31] J. de Oliveira Silva, S.E.M. Miranda, E.A. Leite, A. de Paula Sabino, K.B.G. Borges, V.N. Cardoso, G.D. Cassali, A.G. Guimarães, M.C. Oliveira, A.L.B. de Barros, Toxicological study of a new doxorubicin-loaded pH-sensitive liposome: a preclinical approach, Toxicol. Appl. Pharmacol. 352 (2018) 162–169, https://doi.org/10.1016/j.taap.2018.05.037.

[32] S.E.M. Miranda, J. de, A. Lemos, R.S. Fernandes, J. de, O. Silva, F.M. Ottoni, D. M. Townsend, D. Rubello, R.J. Alves, G.D. Cassali, L.A.M. Ferreira, A.L.B. de Barros, Enhanced antitumor efficacy of lapachol-loaded nanoemulsion in breast cancer tumor model, Biomed. Pharmacother. 133 (2021), 110936, https://doi.org/10.1016/j.biopha.2020.110936.

[33] S. Honary, F. Zahir, Effect of zeta potential on the properties of nano-drug delivery systems - a review (Part 1), Trop. J. Pharm. Res. 12 (2013) 255–264, https://doi.org/10.4314/tjpr.v12i2.19.

[34] D.C. Drummond, C.O. Noble, Z. Guo, K. Hong, J.W. Park, D.B. Kirpotin, Development of a highly active nanoliposomal irinotecan using a novel intraliposomal stabilization strategy, Cancer Res. 66 (2006) 3271–3277, https://doi.org/10.1158/0008-5472.CAN-05-4007.

[35] A. Casadó, M. Mora, M.L. Sagristá, S. Rello-Varona, P. Acedo, J.C. Stockert, M. Cañete, A. Villanueva, Improved selectivity and cytotoxic effects of irinotecan via liposomal delivery: a comparative study on Hs68 and HeLa cells, Eur. J. Pharm. Sci. 109 (2017) 65–77, https://doi.org/10.1016/j.ejps.2017.07.024.

[36] D.R. Khan, M.N. Webb, T.H. Cadotte, M.N. Gavette, Use of targeted liposome-based chemotherapeutics to treat breast cancer: supplementary issue: Targeted therapies in breast cancer treatment, Breast Cancer Basic Clin. Res. 9 (2015) 1–5, https://doi.org/10.4137/BCBCR.S29421.

[37] S. Al-Mahmood, J. Sapiezynski, O.B. Garbuzenko, T. Minko, Metastatic and triple-negative breast cancer: challenges and treatment options, Drug Deliv. Transl. Res. 8 (2018) 1483–1507, https://doi.org/10.1007/s13346-018-0551-3.

[38] D.B. Fenske, P.R. Cullis, Liposomal nanomedicines, Expert Opin. Drug Deliv. 5 (2008) 25–44, https://doi.org/10.1517/17425247.5.1.25.

[39] K. Ghosh, C.K. Thodeti, A.C. Dudley, A. Mammoto, M. Klagsbrun, D.E. Ingber, Tumor-derived endothelial cells exhibit aberrant Rho-mediated mechanosensing and abnormal angiogenesis in vitro, Proc. Natl. Acad. Sci. U. S. A. 105 (2008) 11305–11310. https://doi.org/10.1073/pnas.0800835105.

[40] S.S. Nunes, R.S. Fernandes, C.H. Cavalcante, I. da Costa César, E.A. Leite, S.C. A. Lopes, A. Ferretti, D. Rubello, D.M. Townsend, M.C. de Oliveira, V.N. Cardoso, A.L.B. de Barros, Influence of PEG coating on the biodistribution and tumor accumulation of pH-sensitive liposomes, Drug Deliv. Transl. Res. 9 (2019) 123–130, https://doi.org/10.1007/s13346-018-0583-8.

[41] A.L.B. de Barros, L. das, G. Mota, D.C.F. Soares, M.M.A. Coelho, M.C. Oliveira, V. N. Cardoso, Tumor bombesin analog loaded long-circulating and pH-sensitive liposomes as tool for tumor identification, Bioorg. Med. Chem. Lett. 21 (2011) 7373–7375, https://doi.org/10.1016/j.bmcl.2011.10.016.

[42] A.L.B. De Barros, L. Das Graças Mota, M.M.A. Coelho, N.C.R. Corrêa, A.M. De Góes, M.C. Oliveira, V.N. Cardoso, Bombesin encapsulated in long-circulating pH-sensitive liposomes as a radiotracer for breast tumor identification, J. Biomed. Nanotechnol. 11 (2015) 342–350, https://doi.org/10.1166/jbn.2015.1910.

[43] R.H. Müller, K. Mäder, S. Gohla, Solid lipid nanoparticles (SLN) for controlled drug delivery - a review of the state of the art, Eur. J. Pharm. Biopharm. 50 (2000) 161–177, https://doi.org/10.1016/S0939-6411(00)00087-4.

[44] H. Cheng, J.L. Zhu, X. Zeng, Y. Jing, X.Z. Zhang, R.X. Zhuo, Targeted gene delivery mediated by folate-polyethylenimine-block- poly(ethylene glycol) with receptor selectivity, Bioconjug. Chem. 20 (2009) 481–487, https://doi.org/10.1021/bc8004057.

[45] D.C. Drummond, C. Marx, Z. Guo, G. Scott, C. Noble, D. Wang, M. Pallavicini, D. B. Kirpotin, C.C. Benz, Enhanced pharmacodynamic and antitumor properties of a histone deacetylase inhibitor encapsulated in liposomes or ErbB2-targeted immunoliposomes, Clin. Cancer Res. 11 (2005) 3392–3401, https://doi.org/10.1158/1078-0432.CCR-04-2445.

[46] G. Xu, W. Zhang, M.K. Ma, H.L. McLeod, Human carboxylesterase 2 is commonly expressed in tumor tissue and is correlated with activation of irinotecan, Clin. Cancer Res. 8 (2002) 2605–2611, https://doi.org/12171891.

[47] J. Van Ark-Otte, M.A. Kedde, W.J.F. Van der Vijgh, A.M.C. Dingemans, W.J. M. Jansen, H.M. Pinedo, E. Boven, G. Giaccone, Determinants of CPT-11 and SN-38 activities in human lung cancer cells, Br. J. Cancer 77 (1998) 2171–2176, https://doi.org/10.1038/bjc.1998.362.

[48] M. Han, C.X. He, Q.L. Fang, X.C. Yang, Y.Y. Diao, D.H. Xu, Q.J. He, Y.Z. Hu, W. Q. Liang, B. Yang, J.Q. Gao, A novel camptothecin derivative incorporated in nano-carrier induced distinguished improvement in solubility, stability and anti-tumor activity both in vitro and in vivo, Pharm. Res. 26 (2009) 926–935, https://doi.org/10.1007/s11095-008-9795-9.

[49] H. Kishimoto, M. Momiyama, R. Aki, H. Kimura, A. Suetsugu, M. Bouvet, T. Fujiwara, R.M. Hoffman, Development of a clinically-precise mouse model of rectal cancer, PLoS One 8 (2013), e79453, https://doi.org/10.1371/journal.pone.0079453.

[50] J.C. Castle, M. Loewer, S. Boegel, J. de Graaf, C. Bender, A.D. Tadmor, V. Boisguerin, T. Bukur, P. Sorn, C. Paret, M. Diken, S. Kreiter, Ö. Türeci, U. Sahin, Immunomic, genomic and transcriptomic characterization of CT26 colorectal carcinoma, BMC Genom. 15 (2014) 1–12, https://doi.org/10.1186/1471-2164-15-190.

[51] H. Shinohara, C.D. Bucana, J.J. Killion, I.J. Fidler, Intensified regression of colon cancer liver metastases in mice treated with irinotecan and the immunomodulator JBT 3002, J. Immunother. 23 (2000) 321–331, https://doi.org/10.1097/00002371-200005000-00005.

[52] S.K. Sriraman, G. Salzano, C. Sarisozen, V. Torchilin, Anti-cancer activity of doxorubicin-loaded liposomes co-modified with transferrin and folic acid, Eur. J. Pharm. Biopharm. 105 (2016) 40–49, https://doi.org/10.1016/j.ejpb.2016.05.023.

[53] A. Gabizon, A.T. Horowitz, D. Goren, D. Tzemach, H. Shmeeda, S. Zalipsky, In vivo fate of folate-targeted polyethylene-glycol liposomes in tumor-bearing mice, Clin. Cancer Res. 9 (2003) 6551–6559.

[54] D. Goren, A.T. Horowitz, D. Tzemach, M. Tarshish, S. Zalipsky, A. Gabizon, Nuclear delivery of doxorubicin via folate-targeted liposomes with bypass of multidrug-resistance efflux pump, Clin. Cancer Res. 6 (2000) 1949–1957.

[55] T. Boeing, M.B. Gois, P. de Souza, L.B. Somensi, D. de, M.G. SantAna, L.M. da Silva, Irinotecan-induced intestinal mucositis in mice: a histopathological study, Cancer Chemother. Pharmacol. 87 (2021) 327–336, https://doi.org/10.1007/s00280-020-04186-x.

[56] V. Juang, C.H. Chang, C.S. Wang, H.E. Wang, Y.L. Lo, pH-responsive PEG-shedding and targeting peptide-modified nanoparticles for dual-delivery of irinotecan and microRNA to enhance tumor-specific therapy, Small 15 (2019), 1903296, https://doi.org/10.1002/smll.201903296.